Supporting Information

A hybrid electrolyte for long-life semi-solid-state lithium sulfur batteries

Sui Gu,[a,b,c] *Xiao Huang,* [a,c] *Qing Wang,* [a,c] *Jun Jin,*[a] *Qingsong Wang,*[a,c] *Zhaoyin Wen,*[a,*] *and Rong Qian*[b,*]

[a]CAS Key Laboratory of Materials for Energy Conversion, Shanghai Institute of Ceramics, Chinese Academy of Sciences, Shanghai 200050, P. R. China.

[b]National Center for Inorganic Mass Spectrometry in Shanghai, Shanghai Institute of Ceramics, Chinese Academy of Sciences, Shanghai 200050, P. R. China.

[c]University of Chinese Academy of Sciences, Chinese Academy of Sciences, Shanghai 200050, P. R. China.

KEYWORDS: hybrid electrolyte, lithium sulfur, oxide ceramic, FDE

Corresponding Authors

*E-mail: zywen@mail.sic.ac.cn

*E-mail: qianrong@mail.sic.ac.cn

Tab.S1 Electrochemical performance comparison between LAGP-FDE, reported hybrid electrolytes and FDE liquid electrolyte.

Electrolytes	Sulfur loading	Current density	Initial capacity	Capacity retention		Ref.
				Retention	Cycles	
LATP-THF	0.2 M Li_2S	0.05 C	924 mAh g^{-1}	900 mAh g^{-1}	150	1
LATP-DOL/DME	~2 M Li_2S_6	0.1 C	978 mAh g^{-1}	750 mAh g^{-1}	50	2
LYZP-DOL/DME	~0.25 M Li_2S_6	0.2 C	950 mAh g^{-1}	850 mAh g^{-1}	150	3
LAGP-DOL/DME	~1 g cm^{-2} S_8	0.2 C	1386 mAh g^{-1}	720 mAh g^{-1}	40	4
FDE	**~1 g cm^{-2} S_8**	**0.2 C**	**1458 mAh g^{-1}**	**910 mAh g^{-1}**	**50**	5
LAGP-FDE	**~1 g cm^{-2} S_8**	**0.1 C**	**1478 mAh g^{-1}**	**1315 mAh g^{-1}**	**50**	**MS**
		1.0 C	**915 mAh g^{-1}**	**668 mAh g^{-1}**	**1200**	

Experimental Section

Preparation of LAGP and LLZTO ceramics: The ceramic $Li_{1.5}Al_{0.5}Ge_{1.5}(PO_4)_3$ (LAGP) was prepared by conventional solid-state reaction method. Stoichiometric amounts of $LiOH•H_2O$, Al_2O_3 (γ-phase), GeO_2, and $(NH_4)H_2PO_4$ were mixed and ground for 8 h in a planetary ball mill. The ground materials were heated at 700 °C for 4 h, followed by a second ball milling and heating at 800 °C for 6 h to obtain pure LAGP powder. The powder was ball-milled for 12 h to obtain the fine ceramic precursor powders. Then the powders were pressed into pellets and sintered at 820 °C for 2 h. All of the above heat treatments were conducted in the ambient atmosphere. The as-obtained Li^+ conductivity of the LAGP ceramic was about 2.4×10^{-4} S cm^{-1}. The preparation of LLZTO ($Li_{6.4}La_3Zr_{1.4}Ta_{0.6}O_{12}$) has been previously reported and the Li^+ conductivity of the LLZTO ceramic was about 6.5×10^{-4} S cm^{-1}.[6]

Preparation of liquid electrolytes: The common ether-based liquid electrolyte was composed of 1 M Lithium bis(trifluoromethanesulfonyl)imide (LiTFSI, Sigma Aldrich)

in 1,3-dioxolane (DOL, Sigma Aldrich, boiling point: 75 °C, flashing point: 1 °C) and 1,2-dimethoxyethane (DME, Sigma Aldrich, boiling point: 85 °C, flashing point: 0 °C) (v/v= 1: 1). The FDE (1,3-(1,1,2,2-Tetrafluoroethoxy) propane (FDE), Hengtong Fluorine, boiling point: 169 °C, flashing point: 69 °C) electrolytes were prepared by dissolving 1 M LiTFSI in a mixed solvent of FDE, DOL, and DME. The ratio of DOL: DME was fixed at 1:1 while FDE was tuned from 80 to 90 vol% (The low content of FDE electrolyte has been previously studied.[5])

Preparation of sulfur cathode: The cathode slurry was prepared by mixing 80 wt% S/KB (Ketjen Black) composites (w/w= 6: 4), 10 wt% acetylene black, 5 wt% carboxymethyl cellulose, and 5 wt% styrene–butadiene rubber by ball milling. Then the slurry was cast onto an aluminum foil substrate. After evaporation of the solvent water, the as-prepared cathode was cut into circular disks with 12 mm in diameter and dried for 12 h at 60 °C under vacuum. The typical sulfur loading was about 1 mg cm^{-2}. The high sulfur loading of S/C cathodes was about 3.0 mg cm^{-2}.

Assembly and electrochemical characterization of semi-solid-state Li-S batteries: The inorganic ceramic (LAGP, LLZTO) was used as the solid electrolyte. Commercially available glassy fibers soaked with liquid electrolytes (40 ul) were stuck to the ceramics closing to the cathode and anode, respectively. CR2025-type coin cells were assembled in an argon-filled glove box (oxygen and water contents less than 1 ppm) containing lithium foils as both the counter and reference electrodes. The soft-package Li-S batteries with same configuration were sealed using a plastic film in an argon-filled glove box. Batteries were galvanostatically cycled on an LAND CT2001A battery test

system (Wuhan, China) at current densities mentioned in the discussion. The electrochemical impedance spectroscopy (EIS) measurements were performed on an Autolab PGSTAT302N Electrochemical Workstation (ECO CHEMIE B.V, Netherlands) from 1 MHz to 0.1 Hz with an amplitude of 10 mV.

Characterization methods: The Li^+ transference number of liquid electrolyte was obtained by direct-current (DC) polarization measurements and combining alternating-current (AC) impedance using a symmetric Li/electrolyte/Li batteries.[7] The ionic conductivity of ceramics and hybrid electrolytes were obtained by AC impedance analysis using a symmetric batteries with stainless steel as reference electrodes. Powder X-ray diffraction (Rigaku) was employed to determine the phase component of ceramics at room temperature. SEM microscopy (Hitachi S-4800) was used to study the morphology of Li anodes and ceramics. X-ray photoelectron spectroscopy (XPS) analyses were performed (Thermo scientific ESCALAB 250) to confirm the sulfur environment of discharged cathodes. The samples of lithium anode for SEM and S/C cathode for XPS were stored in an argon-filled box and transferred into sample chambers without exposure to air.

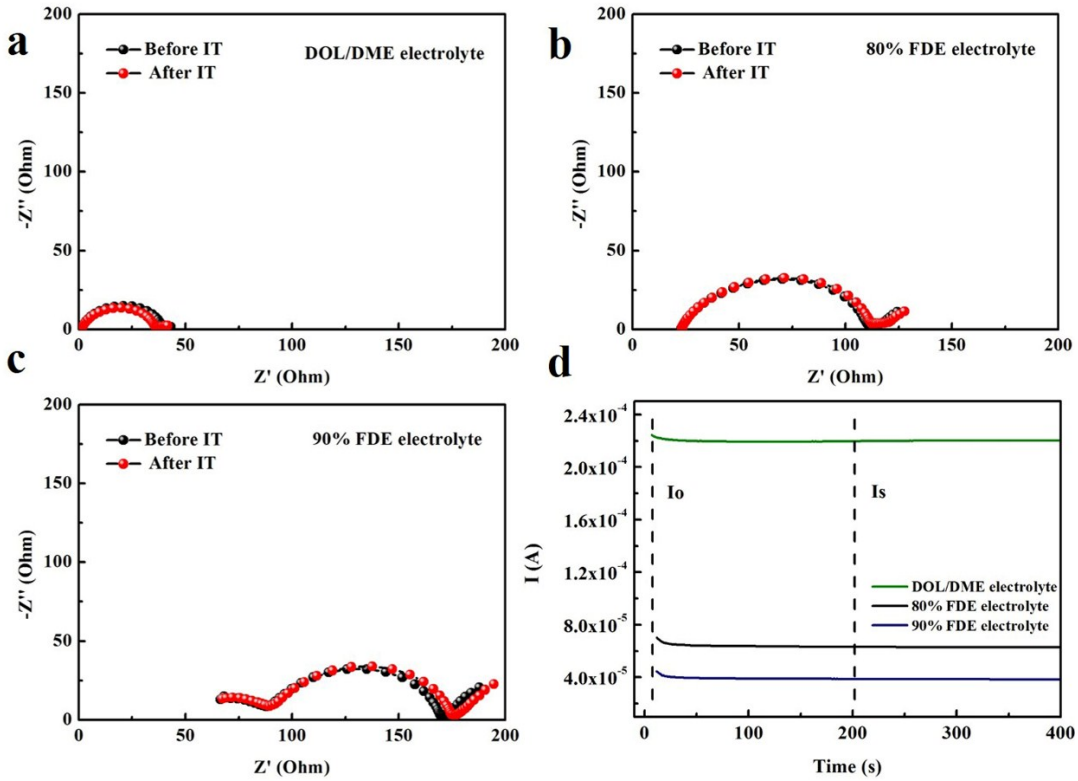

Fig.S1 a-c. Nyquist plots of the Li/electrolyte/Li cells before polarization and after polarization. **IT**: direct-current polarization. **d.** Room temperature chronoamperometry of the Li/electrolyte/Li cells at a potential of 10 mV.

The Li^+ transference number was calculated by the formula:[7]

$$t_+ = \frac{I_s R_{bs}(\Delta V - I_o R_{po})}{I_o R_{bo}(\Delta V - I_s R_{ps})}$$

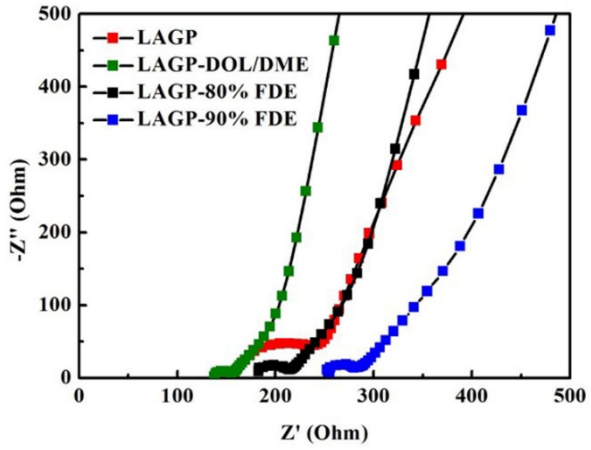

Fig.S2 Nyquist plots of the symmetrical cells based on different hybrid electrolyte with stainless steel electrodes.

Tab.S2 Parameters and ionic conductivities of the hybrid electrolytes and LAGP ceramic.

Samples	h/mm	d/mm	R/ohm	σ/S cm^{-1}
DOL/DME-LAGP	1	13.4	157.3	4.5*10^{-4}
80% FDE-LAGP	1	13.5	214.3	3.2*10^{-4}
90% FDE-LAGP	1	13.5	280.3	2.5*10^{-4}
LAGP	0.8	13.3	240.0	2.4*10^{-4}

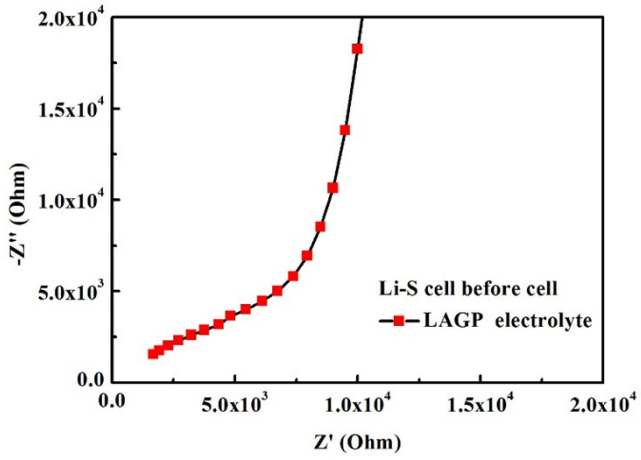

Fig.S3 Nyquist plots of all-solid-state Li-S batteries with LAGP ceramics.

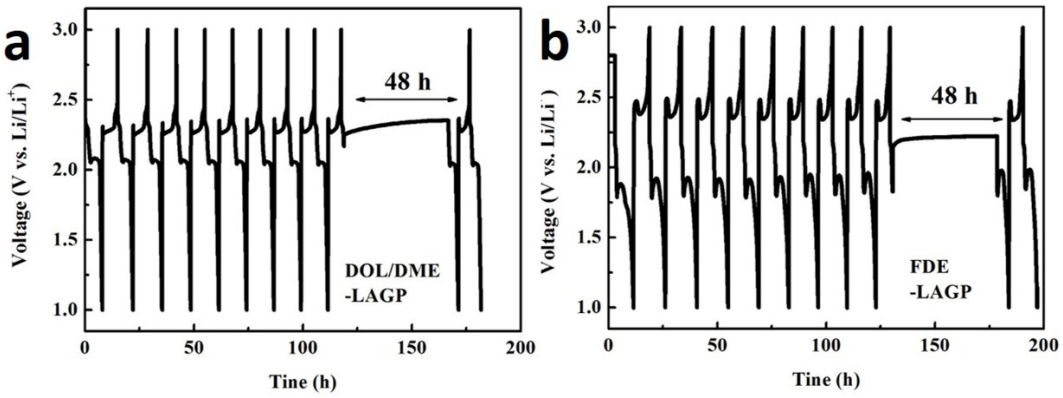

Fig.S4 The galvanostatic charge-discharge curves as a function of time for semi-solid-state Li-S batteries. **a.** DOL/DME-LAGP electrolyte. **b.** FDE-LAGP electrolyte.

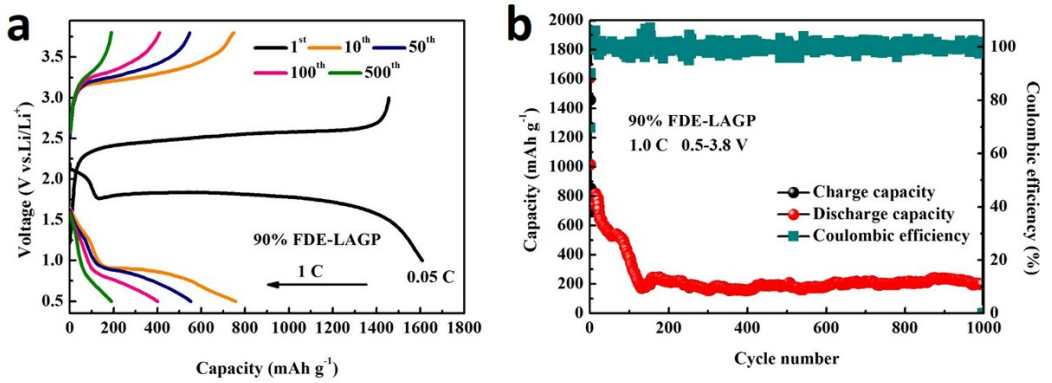

Fig.S5 Semi-solid-state Li-S battery performance with 90%FDE-LAGP electrolyte. **a.** Charge-discharge voltage profiles. **b.** Long-term cycling performance at 25 °C and 1 C.

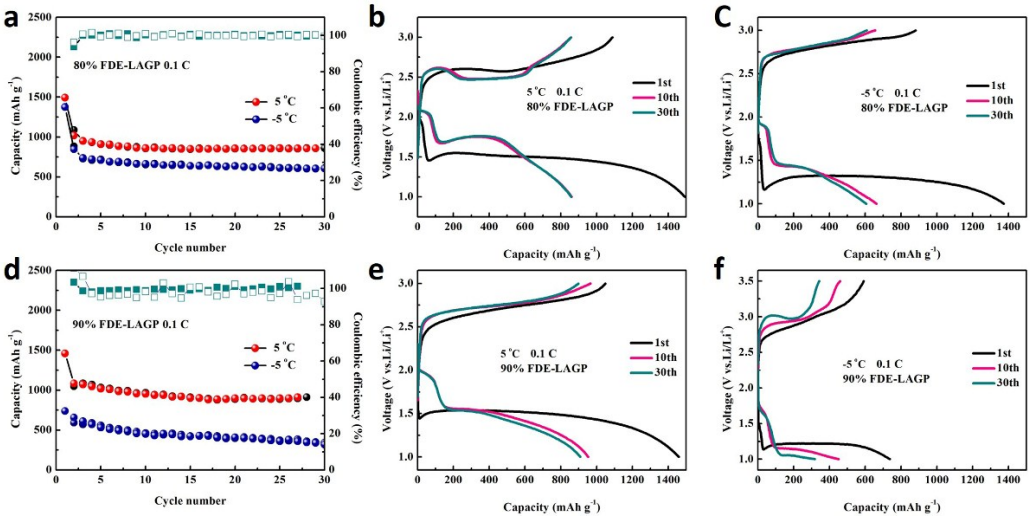

Fig.S6 Low-temperature semi-solid-state Li-S batteries at 5 °C, -5 °C and 0.1 C. Cycle stability, voltage profiles with **a-c)** 80%FDE-LAGP electrolyte and **d-f)** 90%FDE-LAGP electrolyte.

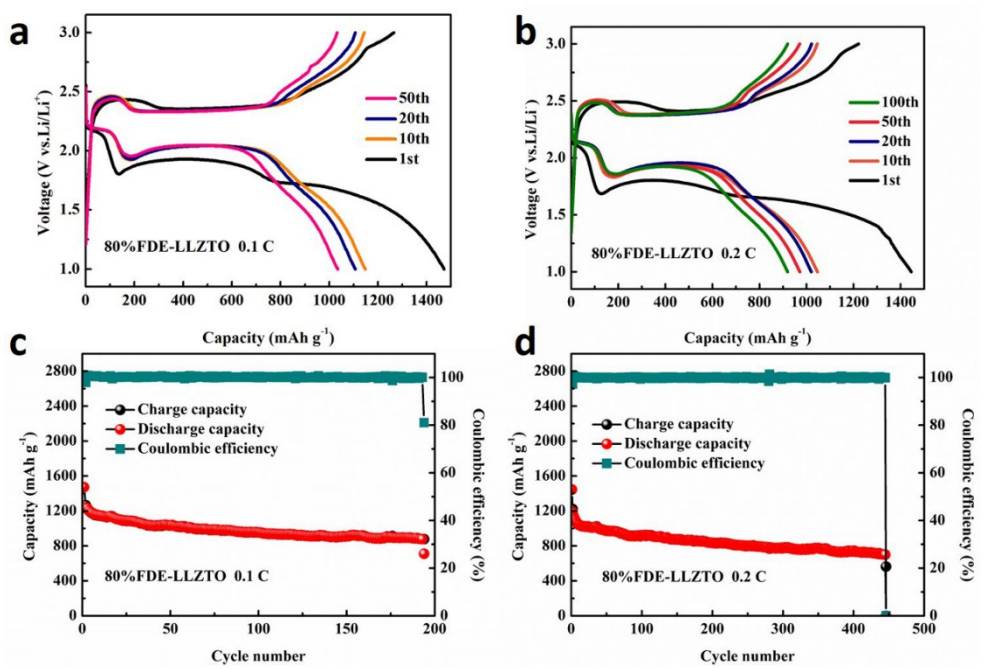

Fig.S7 Semi-solid-state Li-S battery performance with 80%FDE-LLZTO electrolyte at 25 °C. **a-b)** Voltage profiles and **c-d)** Cycling performance at 0.1 C and 0.2 C, respectively.

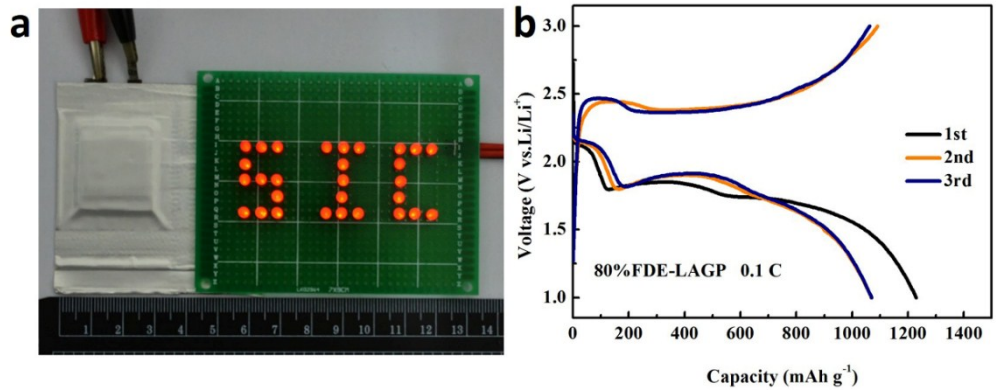

Fig.S8 a. Digital photo of soft-package semi-solid-state Li-S batteries (2.5cm x 2.5cm) with 80%FDE-LAGP hybrid electrolyte. **b.** The charge-discharge voltage profiles at 25°C.

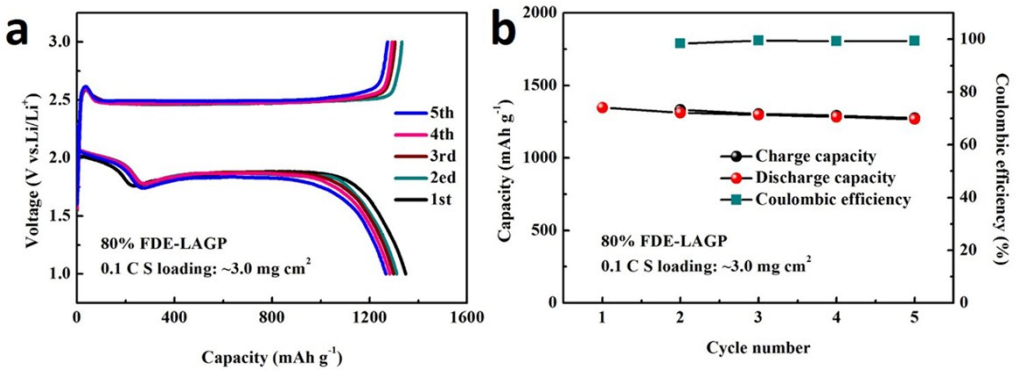

Fig.S9 Semi-solid-state Li-S battery performance with a high sulfur loading of about 3.0 mg cm^{-2} at 25°C.

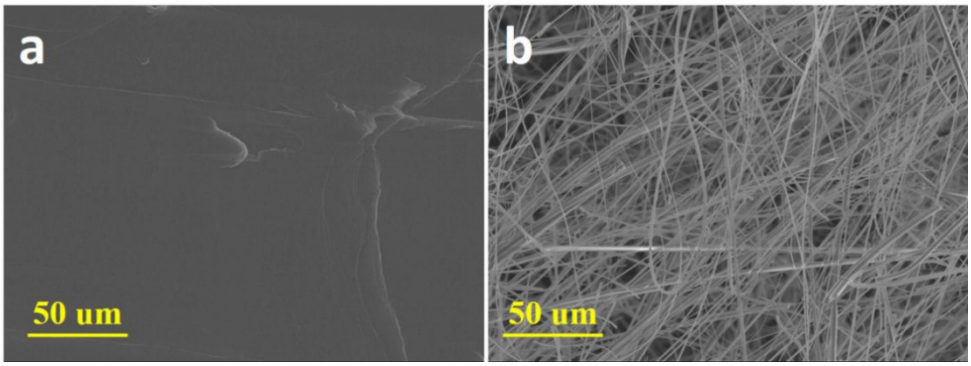

Fig.S10 SEM images of pristine Li foil **(a)** and glass fiber **(b)**.

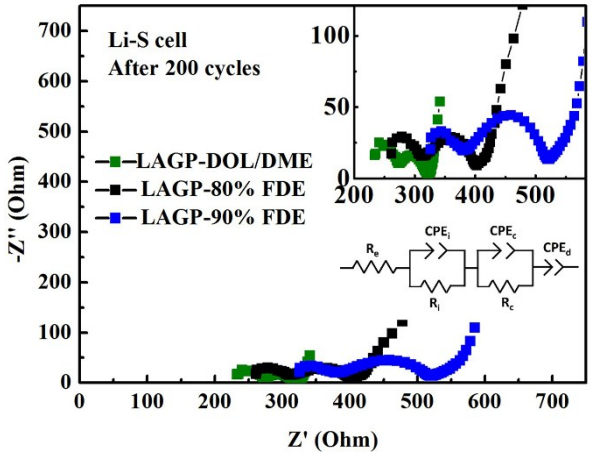

Fig.S11 Nyquist plots of Li-S batteries with hybrid electrolytes after 200 cycles. The inset is the equivalent circuit model.

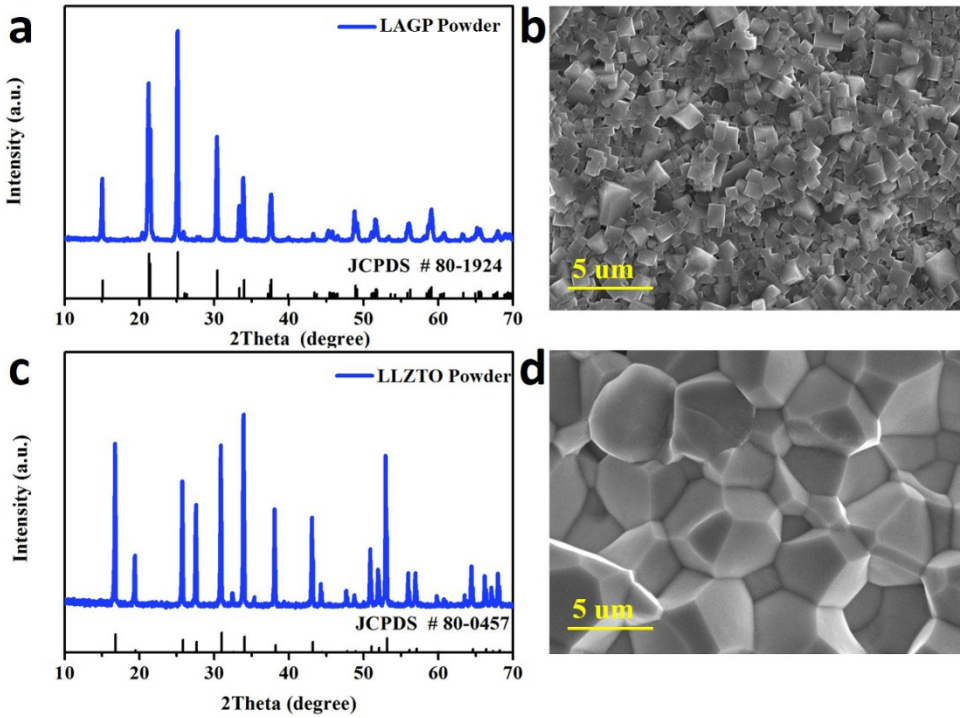

Fig.S12 XRD pattern of prepared LAGP **(a)** and LLZTO **(c)** powders and SEM image of pristine LAGP **(b)** and LLZTO **(d)** ceramic.

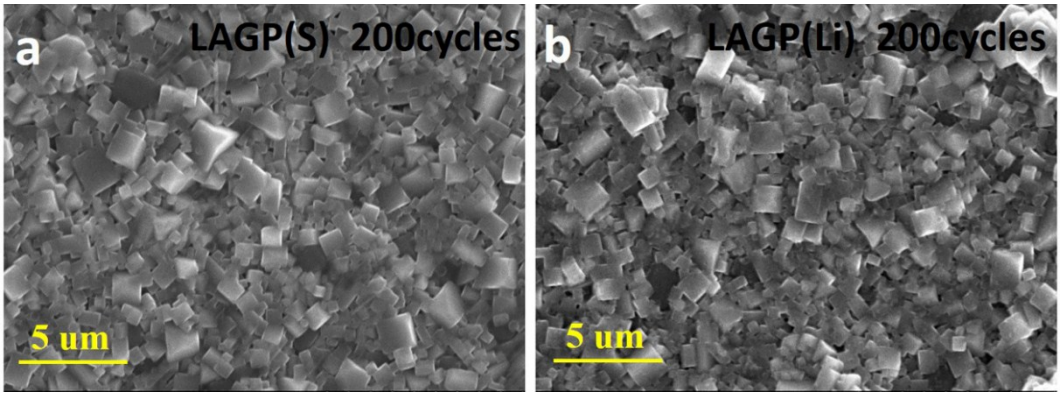

Fig.S13 SEM images of LAGP ceramics after 200 cycles. **a.** Close to S/C cathode side. **b.** Close to Li anode side.

References

1 L. Wang, Y. G. Wang and Y. Y. Xia, *Energy Environ. Sci.*, 2015, **8**, 1551-1558.

2 S. Wang, Y. Ding, G. Zhou, G. Yu and A. Manthiram, *ACS Energy Letters*, 2016, **1**, 1080-1085.

3 X. Yu, Z. Bi, F. Zhao and A. Manthiram, *Adv. Energy Mater.*, 2016, **6**, 1601392.

4 Q. S. Wang, J. Jin, X. W. Wu, G. Q. Ma, J. H. Yang and Z. Y. Wen, *Phys. Chem. Chem. Phys.*, 2014, **16**, 21225-21229.

5 S. Gu, R. Qian, J. Jin, Q. S. Wang, J. Guo, S. P. Zhang, S. J. Zhuo and Z. Y. Wen, *Phys. Chem. Chem. Phys.*, 2016, **18**, 29293-29299.

6 X. Huang, C. Shen, K. Rui, J. Jin, M. Wu, X. Wu and Z. Wen, *JOM-J. Miner. Met. Mater. Soc.*, 2016, **68**, 2593-2600.

7 K. M. Abraham, Z. Jiang and B. Carroll, *Chem. Mat.*, 1997, **9**, 1978-1988.